






## Article

# Distribution Dynamics of *Diplopanax stachyanthus* Hand.-Mazz. (Mastixiaceae) and Its Implications in Relict Mastixioid Flora Conservation

Menglin Chen <sup>1,2,3,4,†</sup> , Yongjingwen Yang <sup>1,2,3,4,†</sup> , Lin Lin <sup>1,4</sup> , Yunhong Tan <sup>2,3</sup> , Min Deng <sup>1,4,\*</sup>  and Yunjuan Zuo <sup>2,3,\*</sup>

- <sup>1</sup> Yunnan Key Laboratory of Plant Reproductive Adaptation and Evolutionary Ecology, Institute of Biodiversity, School of Ecology and Environmental Science, Yunnan University, Kunming 650500, China; chenmenglin@xtbg.ac.cn (M.C.); yangyongjingwen@gmail.com (Y.Y.); linlin.ynu@gmail.com (L.L.)
- <sup>2</sup> Southeast Asia Biodiversity Research Institute, Chinese Academy of Sciences & Center for Integrative Conservation, Xishuangbanna Tropical Botanical Garden, Chinese Academy of Sciences, Menglun 666303, China; tyh@xtbg.org.cn
- <sup>3</sup> Yunnan International Joint Laboratory of Southeast Asia Biodiversity Conservation, Menglun 666303, China
- <sup>4</sup> The Key Laboratory of Rare and Endangered Forest Plants of National Forestry and Grassland Administration & The Key Laboratory for Silviculture and Forest Resources Development of Yunnan Province, Yunnan Academy of Forestry and Grassland, Kunming 650201, China
- \* Correspondence: dengmin@ynu.edu.cn (M.D.); zuoyunjuan@xtbg.ac.cn (Y.Z.); Tel.: +86-136-6172-0514 (M.D.); +86-159-2118-3248 (Y.Z.)
- † These authors contributed equally to this work.

**Abstract:** Climate is a key driver shaping the distribution pattern of organisms. Cenozoic climate change has led to extensive biota turnover. Untangling the distribution dynamics of a representative lineage of flora can provide deep insights into biodiversity conservation. *Diplopanax* is a notable relict lineage of the Tertiary mastixioid flora with abundant fossils in the Northern Hemisphere. *Diplopanax stachyanthus* Hand.-Mazz. is a representative relict lineage of the mastixioid flora, which was once widespread in the Northern Hemisphere of the early Tertiary period, but with only endemic distribution in the (sub)tropical humid forests of East Asia. It offers a unique chance to understand how climatic drivers shape the Boreotropical flora. In this research, we investigated the distribution dynamics of *D. stachyanthus* at the last glacial maximum (LGM), mid-Holocene (MH), current, and three periods of the future (2041–2060, 2061–2080, and 2081–2100) at four shared socio-economic emissions scenarios pathways. Our results indicated that the Precipitation of the Wettest Quarter (32.6%), the Precipitation of the Driest Quarter (21.2%), and the Precipitation of the Coldest Quarter (17.3%) are the key factors affecting its distribution. The current high suitable distribution areas are primarily in southern China and northern Indo-China. The enforced winter monsoon seasons in East Asia since the late Pliocene period are the key climatic drivers reducing its once widespread distribution in the Northern Hemisphere. Under future scenarios, centroid transfer analysis suggests that its distribution center will shift southwestward, but the potentially suitable habitats in the coastal regions of southern China and northern Indo-China will be lost. These coastal populations should be prioritized for ex situ conservation. Expanding the nature reserve within its long-term stable distribution range in southwest China is an effective strategy for the in situ conservation of the ancient mastixioid flora.

**Keywords:** mastixioids; tertiary relict plant; species distribution modeling; conservation



**Citation:** Chen, M.; Yang, Y.; Lin, L.; Tan, Y.; Deng, M.; Zuo, Y. Distribution Dynamics of *Diplopanax stachyanthus* Hand.-Mazz. (Mastixiaceae) and Its Implications in Relict Mastixioid Flora Conservation. *Forests* **2024**, *15*, 766. <https://doi.org/10.3390/f15050766>

Academic Editors: Nadezhda Tchekakova and Sergey V. Verkhovets

Received: 7 April 2024  
Revised: 22 April 2024  
Accepted: 24 April 2024  
Published: 27 April 2024



**Copyright:** © 2024 by the authors. Licensee MDPI, Basel, Switzerland. This article is an open access article distributed under the terms and conditions of the Creative Commons Attribution (CC BY) license (<https://creativecommons.org/licenses/by/4.0/>).

## 1. Introduction

Climate plays a pivotal role in shaping the distribution patterns of organisms [1]. In the future, drastic climate fluctuations will affect the suitable distribution areas of species, leading to habitat fragmentation and intensifying biodiversity loss [2–4]. The Sixth

Assessment Report of the IPCC underscores that, unless there is a marked reduction in global greenhouse gas emissions, the objective of constraining warming to below 2 °C will remain unattainable [5]. Earlier research has indicated that a 2 °C temperature increase may result in a 16% reduction in distribution areas [6] and an increasing risk of species extinction [7–9]. The upsurge in anthropogenic climate change has accelerated habitat loss and fragmentation, especially for endangered species [10].

The warm and humid climate of the Northern Hemisphere during the Early Tertiary period once maintained a large number of plant species distributed in mid-to-high latitudes and around the north [11]. Cenozoic climate change, especially Quaternary glaciation, caused Tertiary relict plants to retreat to the three major glacial refuge areas in East Asia, North America, and southwestern Europe [12,13].

Species adjust their distribution areas in response to climate change to ensure the continuation of their lineage [14]. For example, during the Late Cretaceous and Paleogene periods, Ginkgoes were widely distributed in the high-latitude regions of the Eurasian continent. However, as the climate changed, by the late Miocene period, Ginkgoes had become extinct in North America, followed by their disappearance from Europe after the Pliocene [15]. Subsequently, due to the effects of the Quaternary glaciation, the current distribution patterns were gradually formed. Similar situations occurred in the distribution range formation processes of *Davidia* [16,17] and *Cathaya* [18]. During the Paleocene–Eocene period, the earth was generally much warmer and more humid than today [19]. The Northern Hemisphere experienced a more equable climate, with minimal latitudinal temperature gradients [20]. The Arctic was relatively warm, supporting forests instead of ice caps [21]. Tropical rainforests extended into higher latitudes [22]. Followed by the drastic climate dry and cold shift at the Eocene–Oligocene boundary [23] and the continuous cooling during the Oligocene and the Neogene periods [24], these Boreotropical lineages retreated to the southern refugia and (or) experienced regional extinction resulted in disconnected distribution [24]. Nevertheless, the time and formation of the Northern Hemisphere disjunction concealed a complicated nature, which involved the ancient vicariance, long distance dispersal, or a combination of both [25–28]. All these studies provide a deep understanding of the key drivers that shape the Northern Hemisphere plant diversity pattern.

Among the Northern Hemisphere disjunctions, less attention was placed on the disjunction between the Asian endemic (sub)tropical lineages and their widespread fossils. The masitixioids, also known as Mastixioideae [29], is allied to Cornaceae, with two extant genera of evergreen trees, *Mastixia* Blume and *Diplopanax* Hand.-Mazz. [30,31]. Mastixioids are currently only native to limited areas of Southeast Asia [29]. They are well-known thermophilous plants and usually occur in primary humid subtropical to paratropical broad-leaved evergreen vegetation from a latitude 600–1900 m, generally in moist habitats [31,32]. Currently, due to their fragile climate niche and high productivity, these vegetation have undergone severe degradation and disturbance [33]. The species and quantity of Mastixioid, as well as the distribution range, are constantly shrinking, and some species are on the brink of extinction [34–37]. For instance, *Mastixia caudatilimba* C. Y. Wu ex Soong and *Mastixia trichophylla* W. P. Fang have both been classified as Endangered (EN).

Remarkably, mastixioids once covered much of the Cenozoic Northern Hemisphere [30,38,39]. Fossil mastixioids have a long evolutionary history and a wide distribution in Europe, spanning from the latest Cretaceous to the Pliocene period (65 Ma–3 Ma) [30,40,41]. The lineage showed striking abundance and diversity in the European Eocene of the middle latitudes [42], but the occurrences of the Oligocene are in southern Europe, e.g., Italy [39], probably in response to the cooling and dry shift at the E–O boundary [11,43]. They eventually disappeared in Europe during the Pliocene period [40], probably due to the continuously cooling in the Late Neogene period [44]. In contrast, the North American masitixioid fossils show low species diversity and have been recognized from the Middle and Late Eocene periods in Oregon (as *Mastixicarpum*, [45]), the Late Eocene La Port Flora in California, and the Paleocene and Eocene localities in Wyoming, which indicated that mastixioids were widespread in the early Tertiary period

of western North America [29]. Such wide distribution of mastixioids in both Europe and North America during the Eocene period might have been facilitated by the North Atlantic Land Bridge (NALB) [46,47]. The paleogeographic pattern of the fossils indicated that mastixioids retreated to the southern refugia during the late Neogene period and eventually arrived in Southeast Asia [30,48]. The mastixioids from the middle Miocene to the early Pleistocene period Siwalik sediments in Arunachal Pradesh eastern Himalaya are the southmost fossils ever found and the first recorded in Asia [49]. Due to the numerous occurrences and abundance in the fossil flora, mastixioids have been conventionally used as a proxy to indicate a warm and humid climate tropical climate [30].

The genus *Diplopanax* is restrictively distributed in the primary humid forests of Southern China and northern Vietnam [50–52] with two extant species. *D. stachyanthus* is distributed in southern China and northern Indochina (Figure 1), and *D. vietnamensis* is endemic to Vietnam [29,53].



**Figure 1.** (a). *D. Stachyanthus* habitat (subtropical evergreen broad-leaved forest); (b). *D. Stachyanthus* fruit; (c). *D. Stachyanthus* inflorescence (conical inflorescence).

The fruit morphology of *Diplopanax* is very diagnostic, e.g., the ellipsoidal woody fruits with a single-seeded boat shaped locule (which is C-shaped locule on the transverse section), elongated germination valve and numerous scattered vascular bundles rather than a single pair of ovular bundles [16], which is easily distinguishable. Its fossils were well recognized in a wide stratigraphic range from the Early Eocene to Miocene periods in Europe [30,41,54,55]; and Eocene west North American [29,45,56]. Nevertheless, the key climatic drivers that shape the distribution of the mastixioids are still not well understood, as there are very limited fossil records in Asia, plus complicated tectonic activities along the Tethys seaway and Asian modern monsoon evolutionary process [49,57,58]. Additionally, the species was also included in the IUCN Red List in 1998 and was categorized as Vulnerable (VU) based on criterion A1c [59]. Therefore, *Diplopanax* offered a unique chance to explore the key drivers that shape the distribution dynamics of this ancient tropical mastixioids flora since the Neogene period.

In this study, we employed the Species Distribution Models (SDMs), paleoclimate and paleogeographic database to simulate the distribution dynamics of *Diplopanax* at the last glacial maximum (LGM), mid-Holocene (MH), and current and future periods, aiming to: (1) untangle the key climatic factors that affect the distribution of *D. stachyanthus*; and (2) predict the spatial distribution dynamics of *D. stachyanthus* at different geological times. This study can improve our understanding of the impacts of the climate change on the relic plants in the Asian tropical rainforests and can provide a deep insight into how the climatic



drivers have shaped the current distribution of the mastixioid flora for better conservation and forest management in the future.

## 2. Materials and Methods

### 2.1. Study Region

The modern center of the suitable habitat of *D. stachyanthus* is in South China and Southwest China, extending to northern Vietnam and northern Myanmar. Given the large size and limited dispersal ability of *D. stachyanthus*, we have confined the expansion range of the species to within 5° of its distribution boundaries. The study region was defined using species occurrence data, ranging from 92° E to 123° E and from 10° N to 32° N (Figure 2). The study area is located in the Indian monsoon region, characterized by distinct seasonal variations, including alternating monsoon wind directions, hot and humid summers, as well as dry and cool winters [60].

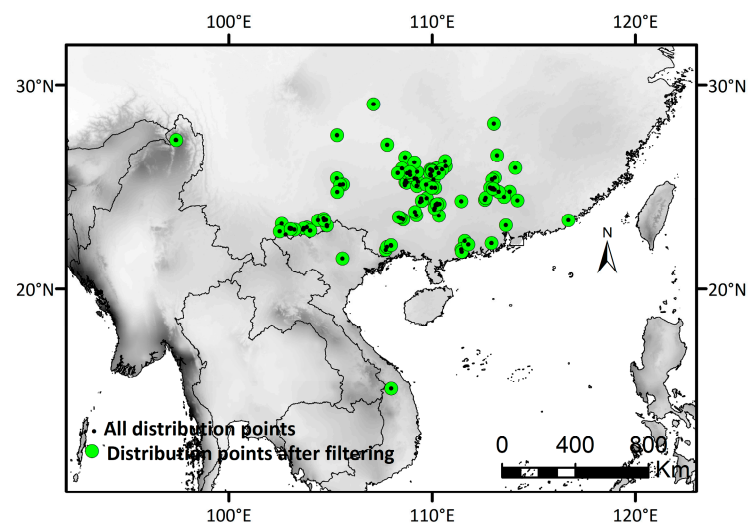


**Figure 2.** Research area and distribution records of *D. stachyanthus*. Black dots represent all the distribution points, and green dots represent distribution points after filtering.

### 2.2. Distributional Records of Species and Bioclimatic Variables

#### 2.2.1. Occurrence Records

Occurrence data were obtained from the Global Biodiversity Information Facility (GBIF; <https://www.gbif.org/> (accessed on 15 August 2023)), the Chinese Virtual Herbarium (CVH; <https://www.cvh.ac.cn/> (accessed on 15 August 2023)), and our field collection records. For those specimen records without coordinates (longitude and latitude), we manually verified the specific collection location and supplemented the relevant information using Google Earth v2017. We checked the specimen information, deleted duplicate records and specimen records with identification errors, and used a total of 305 distribution records for subsequent analysis (Table S1 and Figure 2). The strong correlation of biological distribution data might cause the deviation in simulative results [61]. In R v4.2.2, we utilized the d'ismo' package [62] to randomly retain one point within each  $0.2^\circ \times 0.2^\circ$  grid, aiming to reduce the excessive correlation caused by closely located distribution points. Finally, 84 distribution records were reserved for subsequent analysis (Table S1 and Figure 2).

#### 2.2.2. Selection of Bioclimatic Factors

The 19 bioclimatic variables for each period were downloaded from WorldClim (<https://www.worldclim.org> (accessed on 15 August 2023); 2.5 arc min resolution). Data for the Last Glacial Maximum (LGM) and Mid-Holocene (MH) were sourced from version 1.4, while data for other periods are from version 2.1. The current bioclimatic data uses the average values from 1970 to 2000 [63,64]. GCMEval [65] was used to select the three best-performing global climate models, BCC-CSM2-MR, MIROC6 and MPI-ESM1-2-LR



from the Climate Model Intercomparison Project sixth (CMIP6) [66,67]. To reduce the uncertainty associated with specific models [68], we used the average model of the three models to predict the potential distribution of *D. stachyanthus* for the following three periods (2041–2060, 2061–2080 and 2081–2100) under four shared socio-economic emissions scenarios pathways (SSP1-2.6, SSP2-4.5, SSP3-7.0 and SSP5-8.5). The potential habitat of *D. stachyanthus* during the LGM and MH periods was predicted using the average of the MPI-ESM-P, MIROC-ESM, and CCSM4 models.

### 2.3. Bioclimatic Variable Selection

To avoid the overfitting problem caused by multicollinearity between climate variables [69], we performed environmental variable contribution and Pearson correlation analyses on bioclimatic variables in R v4.1.0. We retained variables with correlation coefficients  $|r| < 0.8$  [70] and observed that some environmental factors had correlation coefficients exceeding  $|0.8|$ . In response, only one variable with a higher contribution was retained and employed in the SDMs [71,72]. For subsequent analysis, six variables were selected to predict the distribution of *D. stachyanthus* (Tables S2 and S3).

### 2.4. Model Configuration and Selection

To select the optimal model for species distribution modeling, an evaluation of the performance of 21 ecological niche models within the *sdm* package [73] in R was conducted (Table S4). All models used 70% of the distribution data as the training set and the remaining 30% as the test set, with 10 replicates and cross-validation as the run type. The training dataset was used for model calibration, and the testing dataset was used for cross-validation of the model evaluation during the calibration process. We evaluated the performance of the models by actively employing the area under the receiver operating characteristic curve (AUC) and the accurate skill statistic (TSS) [74], where higher AUC and TSS values indicated higher accuracy. When the AUC > 0.9 and the TSS > 0.6, the model performance is considered excellent [75,76]. Random forest (RF) was the model with the highest AUC and TSS values and was, therefore, selected for the subsequent SDM analysis (Table S4).

### 2.5. Suitability Level Classification and Spatial Changes

In ArcGIS 10.8 [77], we imported the ASCII format results of the distribution areas predicted by RF for each period, facilitating calculation and comparison. Based on the predicted species existence probability values from RF (0–1), the distribution results were reclassified into four regions as follows: no-suitable habitat (0–0.1); low-suitability habitat (0.1–0.3); medium-suitability habitat (0.3–0.6); and high-suitability habitat (0.6–1) [70,78,79]. Subsequently, we utilized SDMtoolbox 2.0 [80] within ArcGIS to analyze the expansion/contraction of the distribution area and converted Maxent's predicted map into a binary grid layer (unsuitable: 0; suitable: 1). Analyzing the potential distribution of suitable/unsuitable areas under four climate scenarios during different periods, we identified four types of distribution changes: loss, gain, stable, and not suitable [70].

### 2.6. Centroid Shifts

The analysis of centroid position changes in suitable habitats under the four shared socio-economic emissions scenarios during different periods were calculated using the SDMtoolbox.

## 3. Results

### 3.1. Model Performance

The evaluation of 21 models reveals that RF demonstrates the highest AUC and TSS values (AUC = 0.95, TSS = 0.8) (Table S4). Consequently, it is chosen for subsequent *D. stachyanthus* distribution predictions. Based on RF, the known occurrence points of *D. stachyanthus* align well with its predicted suitable habitat during the current time period (Figure 3).

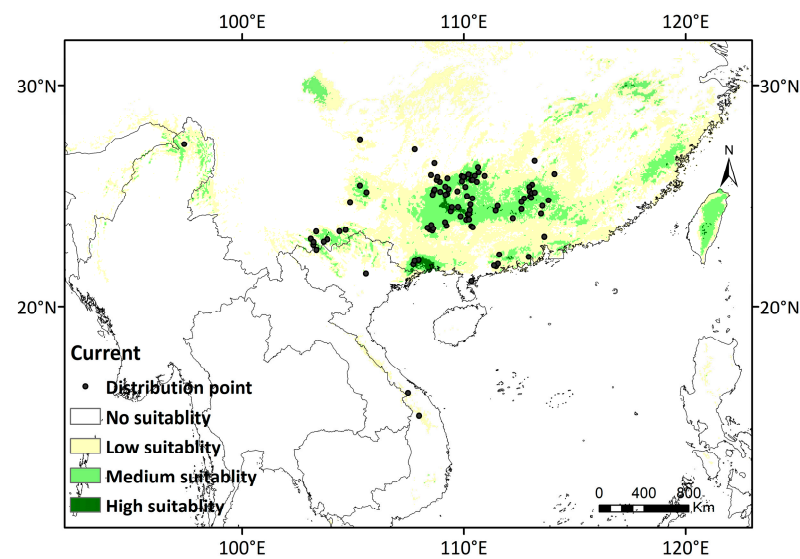


**Figure 3.** Research area and distribution records of *D. stachyanthus*. Black dots represent distribution points after filtering.

### 3.2. Environmental Variable Contribution

The three most influential bioclimatic variables were bio16 (Precipitation of Wettest Quarter) (32.6%), bio17 (Precipitation of Driest Quarter) (21.2%) and bio19 (Precipitation of Coldest Quarter) (17.3%) (Table 1). The total contribution of bioclimatic variables related to precipitation is 71.1%.

**Table 1.** The contribution of environmental variables for predicting the distribution of *D. stachyanthus*.

| Name  | Relative Contribution Rate (%) | Description   |
|-------|--------------------------------|---|
| Bio16 | 32.6                           | Precipitation of Wettest Quarter (mm)                         |
| Bio17 | 21.2                           | Precipitation of Driest Quarter (mm)                          |
| Bio19 | 17.3                           | Precipitation of Coldest Quarter (mm)                         |
| Bio1  | 13.5                           | Annual Mean Temperature(°C)                                   |
| Bio2  | 13.4                           | Mean Diurnal Range (Mean of monthly (max temp–min temp)) (°C) |
| Bio11 | 9.5                            | Mean Temperature of Coldest Quarter (°C)                      |

### 3.3. Potential Distribution of *D. stachyanthus* under Retrospective, Current and Prospective Climate Conditions

The area of highly suitable habitat for *D. stachyanthus* was predicted to be  $0.779 \times 10^4 \text{ km}^2$ , mainly in the Guangxi and Guangdong provinces in China during the LGM (Figure 4a).

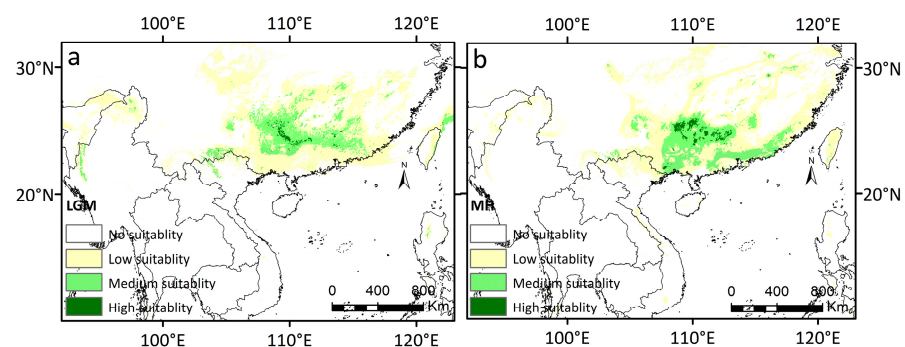


**Figure 4.** The simulated potential distribution areas of *D. stachyanthus* at the geological times. (a) At the LGM; (b) at the MH.

More than 90% of the highly suitable areas are continuously distributed in the Guangxi province. The potential medium suitable area was  $19.807 \times 10^4 \text{ km}^2$ , which is mainly adjacent to the area of high suitability and mainly covers the Guangdong, Guangxi, and Jiangxi provinces of China (Figure 4a). The predicted potential low suitability areas were  $72.477 \times 10^4 \text{ km}^2$ . The area of potential high suitability sharply increased from the LGM to the MH, which was increased by 134.14% and became  $1.824 \times 10^4 \text{ km}^2$  (Figure 4b), and was sporadically distributed at the junction of Guangxi, Guangdong, and Hunan provinces in China. The moderately suitable area was  $20.668 \times 10^4 \text{ km}^2$ , mainly located at the periphery of the highly suitable area in Guangxi and the junction area of the Guangxi, Guangdong, and Hunan provinces (Figure 4b and Table 2).

**Table 2.** The suitable habitats of *D. stachyanthus* predicted by the RF model at different time periods.

| Climate Scenario | Time      | High Suitable ( $10^4 \text{ km}^2$ ) | Medium Suitable ( $10^4 \text{ km}^2$ ) | Low Suitable ( $10^4 \text{ km}^2$ ) | Total ( $10^4 \text{ km}^2$ ) |
|------------------|-----------|---------------------------------------|---|--------------------------------------|-------------------------------|
| SSP1-2.6         | LGM       | 0.779                                 | 19.807                                  | 72.477                               | 90.063                        |
|                  | MH        | 1.824                                 | 20.668                                  | 67.326                               | 89.818                        |
|                  | Current   | 1.113                                 | 20.391                                  | 64.470                               | 85.974                        |
|                  | 2041–2060 | 1.161                                 | 16.292                                  | 66.477                               | 83.931                        |
|                  | 2061–2080 | 0.564                                 | 19.427                                  | 79.066                               | 99.057                        |
| SSP2-4.5         | 2081–2100 | 0.816                                 | 18.335                                  | 57.361                               | 76.512                        |
|                  | 2041–2060 | 0.269                                 | 20.146                                  | 64.641                               | 85.056                        |
|                  | 2061–2080 | 0.092                                 | 18.035                                  | 63.076                               | 81.203                        |
| SSP3-7.0         | 2081–2100 | 0.170                                 | 21.175                                  | 74.519                               | 95.865                        |
|                  | 2041–2060 | 1.248                                 | 18.589                                  | 76.691                               | 96.528                        |
|                  | 2061–2080 | 0.389                                 | 20.503                                  | 57.205                               | 78.097                        |
| SSP5-8.5         | 2081–2100 | 0.234                                 | 18.170                                  | 66.457                               | 84.861                        |
|                  | 2041–2060 | 1.625                                 | 16.359                                  | 69.005                               | 86.990                        |
|                  | 2061–2080 | 0.229                                 | 20.821                                  | 64.898                               | 85.948                        |
|                  | 2081–2100 | 0.719                                 | 16.875                                  | 78.139                               | 95.733                        |

Habitats with potential suitability under current climate conditions are mainly restricted to the mountainous regions along the junction of Guangxi, Guangdong, and Hunan provinces, as well as the southern region of Yunnan (Figure 5).

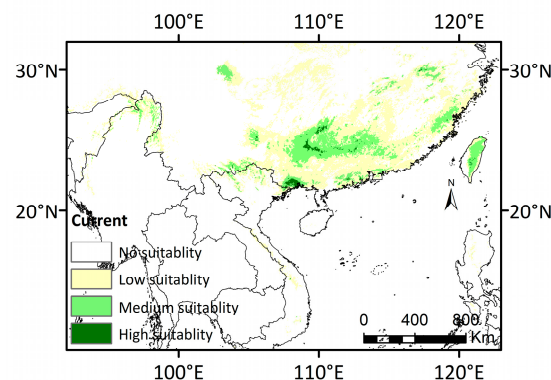


**Figure 5.** Potential distribution map under current climate conditions (1970–2000).

There was scattered distribution in the Fujian and Zhejiang provinces based on our predictions. The habitats with a potentially high suitability were mainly situated in Northern Indo-China, with a total area of only about  $1.113 \times 10^4 \text{ km}^2$ . The predicted distribution range covered the current occurrence sites, including Taiwan Island (Figure 5 and Table 2). The spatial coverage of the moderately suitable region amounted to  $20.391 \times 10^4 \text{ km}^2$ , bordering the highly suitable area. The low-suitability area spanned an area of  $64.470 \times 10^4 \text{ km}^2$ , primarily located in the regions of Guangxi, Guangdong, Yunnan, Hunan, Chongqing, Fujian and Zhejiang, and extended to northern Vietnam and Myanmar



(Figure 5 and Table 2). Overall, the highly suitable and moderately suitable areas were scattered and exhibited an “island-like” discontinuous distribution pattern.

The highly suitable areas under the four climate scenarios showed consistent trends of contraction in the future (Figure 6 and Table 2).

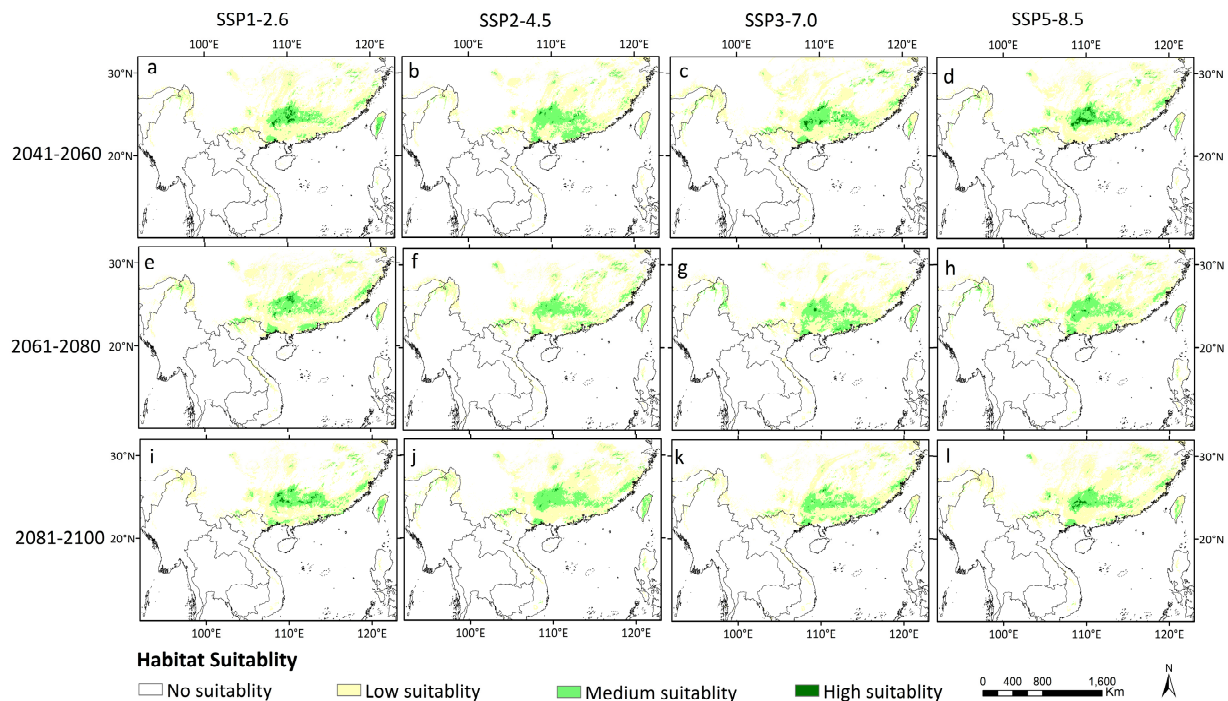


**Figure 6.** Potentially suitable habitats of *D. stachyanthus* under the four shared socioeconomic pathways in the future three periods. (a) SSP1-2.6 2041–2060; (b) SSP2-4.5 2041–2060; (c) SSP3-7.0 2041–2060; (d) SSP5-8.5 2041–2060; (e) SSP1-2.6 2061–2080; (f) SSP2-4.5 2061–2080; (g) SSP3-7.0 2061–2080; (h) SSP5-8.5 2061–2080; (i) SSP1-2.6 2081–2100; (j) SSP2-4.5 2081–2100; (k) SSP3-7.0 2081–2100; (l) SSP5-8.5 2081–2100, respectively.

Overall, the potential distribution area of *D. stachyanthus* was predicted to decrease, with suitable distribution areas mainly concentrated in the Guangdong, Guangxi, Yunnan and Fujian provinces of China, northern Myanmar, and Vietnam. In addition, RF analysis predicted that southern China (especially the Guangdong and Guangxi provinces) had especially connected suitable areas for *D. stachyanthus* (Figure 6).

### 3.4. Distribution Dynamics

By comparing the potential distribution areas from the LGM to the present, our results showed that the total distribution area of *D. stachyanthus* has shown a trend of first increasing and then decreasing (Figure 7).

The species had experienced severe range contraction during MH to the present, with the potential habitats in the eastern coastal areas, large areas in the north, the southwestern peripheral areas, and northern Myanmar contracted. Comparisons of the predicted areas under different paths of sharing scenarios for the present and future periods revealed that the skeletal distribution areas were also more significant than the expanded areas. The overall distribution dynamics still showed a trend of shrinkage in the future (Figure 8).

The predicted expansion areas are mainly distributed in the adjacent areas of the Guangxi, Guizhou, and Yunnan provinces, between the Guangdong and Hunan provinces, and northern Myanmar. The predicted lost areas were mainly in the Guizhou, Hunan, Guangdong, and Guangxi Provinces, as well as large areas of Vietnam. The detailed predicted distribution areas at different geological eras are summarized in Figures 7 and 8.

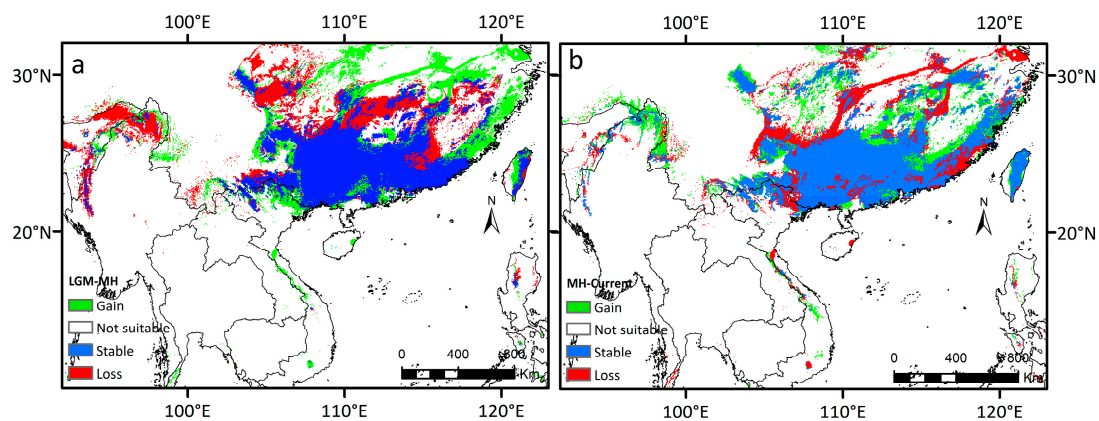


**Figure 7.** Dynamic change map of the potentially suitable area of *D. stachyanthus* at the geological times. (a) at the LGM; (b) at the MH.

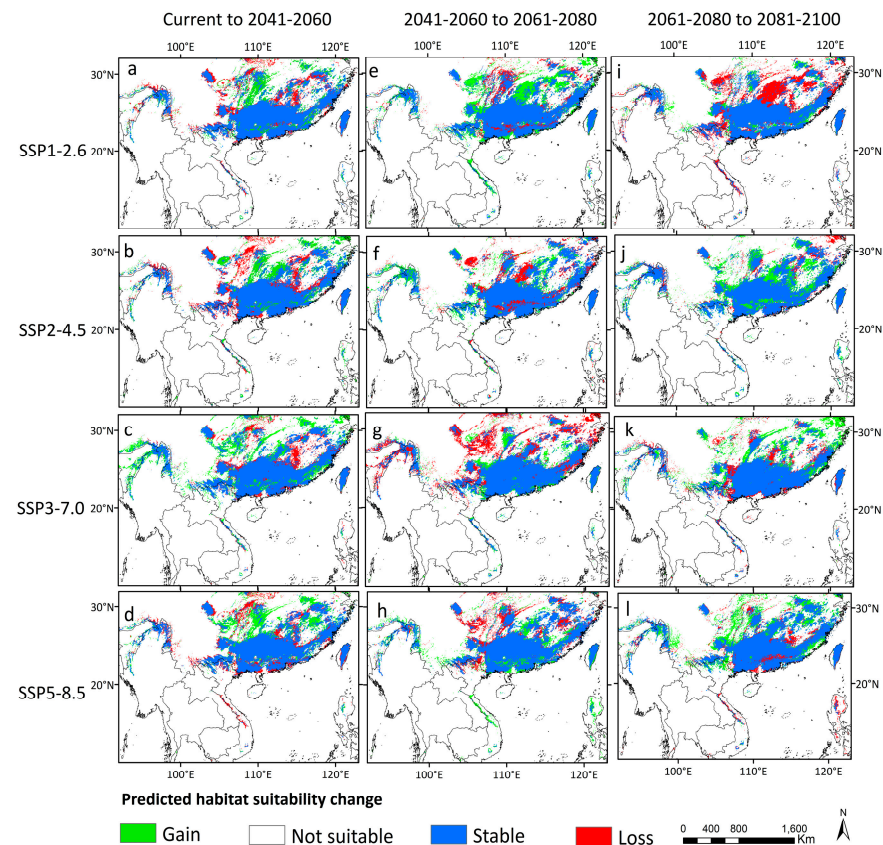


**Figure 8.** Changes in distribution areas of *D. stachyanthus* under different climate scenarios in the next three time periods. (a) current to 2041–2060 SSP1-2.6; (b) current to 2041–2060 SSP2-4.5; (c) current to 2041–2060 SSP3-7.0; (d) current to 2041–2060 SSP5-8.5; (e) 2041–2060 to 2061–2080 SSP1-2.6; (f) 2041–2060 to 2061–2080 SSP2-4.5; (g) 2041–2060 to 2061–2080 SSP3-7.0; (h) 2041–2060 to 2061–2080 SSP5-8.5; (i) 2061–2080 to 2081–2100 SSP1-2.6; (j) 2061–2080 to 2081–2100 SSP2-4.5; (k) 2061–2080 to 2081–2100 SSP3-7.0; (l) 2061–2080 to 2081–2100 SSP5-8.5.

### 3.5. Centroid Shift under the Different Climatic Scenarios

The centroid transfer analysis revealed that the distribution center in Indo-China had minimal migration (Figure S1). Overall, in future scenarios, the center of suitable habitats will initially extend to the southwest. Still, the distance and direction of centroids shift will differ under various CO<sub>2</sub> emission scenarios. Under SSP1-2.6 and SSP2-4.5 plans,

the centroid first moved to the northeast and then southwest, while under SSP3-7.0 and SSP5-8.5 scenarios, the centroid first moves southwest and then northeast.

#### 4. Discussion

##### 4.1. The Primary Climatic Factors Influencing the Distribution of *D. stachyanthus*

Temperature and water availability are the fundamental factors for an organism [81–83]. According to our results, the distribution of *D. stachyanthus* is primarily affected by precipitation as the main climate factor, while temperature serves as a secondary influencing factor. The cumulative contribution ratio of precipitation factors was 71.1% (Table 1), indicating that precipitation stands out as the most pivotal variable. *D. stachyanthus* is distributed in warm and humid mixed evergreens and deciduous broad-leaved forests of mid to high altitude montane areas in southern China [84]. This region is under the Indian summer monsoon regime [85,86]. Summer is warm with sufficient rainfall, which meets the growth needs of *D. stachyanthus* during its growth period [84]. Field observations revealed that most *D. stachyanthus* thrived along riverbanks and valleys. Its fruits are large, averaging 47.97 mm in length, 26.64 mm in diameter, and 16.07 g in weight. They are characterized by a prolonged ripening process and seeds with a hard woody shell that inhibits germination [52,86]. Seedlings or young trees are seldom observed in these forests, suggesting the ageing of the population and regeneration difficulties [87]. Seed germination test indicated that the germination rate of *D. stachyanthus* is only 10% in the wild [84] and only 56% even under controlled conditions (i.e., incubation for 450 days in a humid environment after 165 days of wet sand storage in room temperature) [88]. A long germination period and delayed seed ripening process render this species susceptible to water scarcity. Consequently, drought conditions, likely exacerbated by climate change, may significantly impact the population dynamics and species' distribution range. Similarly, the seed of *Davidia involucrate* Baill necessitates a prolonged moist condition to mitigate the physical barrier presented by the thick woody nutshell. This is crucial for ensuring seed moisture during the extended period of embryo ripening and fruit, thereby diluting the fruit's chemical inhibitors during germination [89,90]. Consequently, optimal humidity levels and a stable environment may be vital for regenerating these Tertiary relict plants of Cornales.

Paleoclimatic reconstructions indicated that the fossils of *Diplopanax* were predominantly located in areas with warm and humid climates. This stable and humid climate has been sustained in Europe from the Eocene period, until the Pliocene period, and in North America until the late Miocene period [41,91–93]. Abundant fossil records have been extensively documented in Europe and North America [29,45,94]. The genus had a broad distribution across North America and Europe during the Paleogene period, coinciding with the warm and humid climate conditions. This was until the late Neogene period, when global climatic cooling and aridification led to habitat fragmentation [13]. Its distribution in Europe persisted until the Pliocene period, as fossils with close affinities to *Dioplopanax* were still found in S. Pedro da Torre deposits (Portugal) [95] and the fossil flora of Turow near Bogatynia (Poland) [48]. This evidence suggested that a warm and humid climate was still prevalent in these regions during the Late Neogene period, and a semiarid shift in these regions was relatively recent [92].

The analysis of 65 relict families in China and their key distribution restricting factors revealed that precipitation is the predominant factor influencing the distribution of over half of the relict plant lineages in China [12], which aligns with *D. stachyanthus*. The intensification of seasonality and the enhancement of the East Asian winter monsoon since the Pliocene period [96] were the primary drivers for the replacement of these relict lineages by the dominant tree species (e.g., Fagaceae, Lauraceae, Theaceae, Magnoliaceae) in East Asian subtropical mixed evergreen and deciduous broad-leaved forests (MEDBFs) in the ecosystems. Future global warming and changes in drought conditions in southern China and northern Indo-China will cause the distribution range of *D. stachyanthus* to shift southwestward into the montane regions. This migration trend is consistent with other relict plants adapted to humid and stable climates, e.g., *Metasequoia* Hu and W.C.Cheng and



*Shaniodendron* M. B. Deng, H. T. Wei and X. Q. Wang [12,97–99], whereas the relict plants sensitive to temperature changes rather than humidity changes will gradually migrate towards higher latitudes in the north [100,101], such as *Alsophila spinulosa* (Wall. ex Hook.) R. M. Tryon [102], and *Metasequoia glyptostroboides* Hu and W. C. Cheng [103].

Despite the varying distribution dynamics of the relict plants, their suitable habitats will steadily diminish due to their narrow ecological niches [12,101]. The rapid climate changes make it impossible for these ancient lineages to adapt to the new environments or disperse to recent locations in a short period.

A growing body of evidence suggests that climatic seasonality variations significantly influence the forest structure and function, especially in mountain ecosystems [104–107]. The importance of temperature seasonality over precipitation seasonality in explaining the total variation of the occurrence of the dominant tree species in East Asian subtropical MEDBFs was detected to be five times greater [108]. The predominant tree species in mixed forests are generally capable of enduring seasonal drought and daily temperature fluctuations [70,109–113]. These dominant species can tolerate a certain degree of low temperatures and possess seasonal drought resistance capability, resulting in a broader distribution range than the relict plants [111]. The increasing and intensified seasonal drought since the late Miocene has driven these dry-tolerant species to become the dominant lineages in MEDBFs [114]. Meanwhile, relict lineages, which exclusively track the warm and humid climates, have been gradually replaced in the forest ecosystem, and their distribution was restricted to very small regions.

#### 4.2. Distribution Dynamics of *D. stachyanthus*

During the Pleistocene period, there were periodic alternations between the glacial and interglacial periods that greatly affected the distribution of plants [14,47]. The last glacial maximum had the most significant impact on the distribution ranges of plants [16,115,116]. During this period, the temperature dropped sharply, and ice sheets covered a large area of the continents [117], forcing the plants to migrate to the southern low latitudes or retreat to the cryptic refugia for survival [98,118]. Our prediction inferred that *D. stachyanthus* had a significant continuous suitable habitat in the subtropics of China during the LGM, with limited fragmentation. East Asia did not experience the development of a continental ice sheet during the LGM [119–121]. The biota was less affected by the climatic extremes at this time [122,123]. The long-term stable climate in East Asian (sub)tropics made these areas a refugia to preserve these ancient lineages [116]. A recent spatial population genetic study on *D. stachyanthus* revealed two main refugia in Southwest and South China [57], consistent with our predicted high suitability regional distribution during the LGM period, indicating that our prediction is accurate.

From the LGM to the MH, the range of highly habitats suitable for *D. stachyanthus* underwent a notable expansion. According to prior research, the extent of monsoon regions and the magnitude of monsoon precipitation in China were both greater during the MH period compared to the LGM. This warmer and wetter climate was more conducive to the survival of *D. stachyanthus*, aligning well with its ecological preferences [124].

Under the future scenarios, the high suitability area of *D. stachyanthus* located at the border between Guangdong and northern Guangxi, Guizhou and Hunan will be maintained. Still, the potential habitat in the coastal areas of southeast China and north Indo-China is expected to be lost. Therefore, there is an urgent need for the ex situ conservation of coastal populations to maintain a high level of genetic diversity of this species.

#### 4.3. Conservation and Forestry Management

*D. stachyanthus*, an endangered species native to China and Northern Vietnam, is currently listed on the IUCN Red List [59]. Our research simulated and predicted the potential distribution of suitable habitats for *D. stachyanthus*. The results suggest that the currently identified highly suitable habitat area for *D. stachyanthus* is  $10.991 \times 10^4 \text{ km}^2$ ,

making up only 7.52% of the overall suitable territory. This area is located at the border between Guangdong, northern Guangxi, and Guizhou, Hunan, and represents a long-term stable distribution area for *D. stachyanthus* in the future. Population genetic studies revealed that populations in this area possess the highest genetic diversity and most private haplotypes, representing a distinct genetic composition [57]. Therefore, the populations in this area should be prioritized for in situ conservation. However, our predictions revealed that the distribution of *D. stachyanthus* in the coastal areas of southeast China and northern Indo-China would decrease in the future. These areas are highly urbanized and severely impacted by human interference. Even the moderately suitable area of *D. stachyanthus* in this region could gradually diminish. Therefore, ex situ conservation is needed to conserve the genetic integrity of *D. stachyanthus*, introducing the populations to botanical gardens and nurseries and transplanting the germplasm to long-term stable similar habitats.

Other mastixioid flora species, which exhibit similar seed characteristics and habitat preferences to *D. stachyanthus* [125], possess narrower distribution ranges and smaller population sizes compared to the latter [126]. *Mastixia euonymoides* Prain, for instance, has been surveyed to reveal merely 10 distinct populations, with its natural population size and scale already falling below the critical threshold of the minimum viable population. Alarmingly, nearly half of its populations lack seedlings, pointing to considerable challenges in natural regeneration. Consequently, these species appear to face a higher level of threat than *D. stachyanthus*, underscoring the urgent need for intensified research efforts in the future to establish a theoretical framework for devising effective conservation strategies.

## 5. Conclusions

The Precipitation of the Wettest Quarter, Precipitation of the Driest Quarter and Precipitation of the Coldest Quarter are the three principal climatic factors that account for over 70% of the distribution pattern of *D. stachyanthus*. This suggests that humidity and stable climate conditions are the significant limiting factors for *D. stachyanthus*. The main areas with highly suitable habitats for *D. stachyanthus* are situated in the south and southwest of China. However, the regions highly suitable for *D. stachyanthus* in the southeast and north are expected to decrease, with the centroids forecasted to shift southwestward. Since *D. stachyanthus* is adapted to highly humid environments, and its seeds are sensitive to drought, these factors may hinder its population regeneration. Given its limited dispersal ability, habitat fragmentation, and anticipated aridification, the threatened status of mastixioid tree species like *D. stachyanthus* might be much higher than previously expected. To secure the long-term survival of *D. stachyanthus* and the ancient mastixioid flora, there are two key strategies suggested: (1) in situ conservation by expanding the protected areas (PA) to cover its future core distribution areas and protecting the long-time stable habitats of *D. stachyanthus*; and (2) ex situ conservation by establishing germplasm collections and transplanting seedlings to their future high-suitability habitats in the southwest.

**Supplementary Materials:** The following supporting information can be downloaded at: <https://www.mdpi.com/article/10.3390/f15050766/s1>, Figure S1. The centroid distribution of *D. stachyanthus* in different periods. Table S1: Distribution records of *Diplopanax stachyanthus*; Table S2: Percent contributions of the bioclimatic in the species distribution models for *Diplopanax stachyanthus*; Table S3: Results of Pearson correlation analysis of 19 bioclimatic variables for *Diplopanax stachyanthus*; Table S4: Evaluation results of species distribution models for *Diplopanax stachyanthus*.

**Author Contributions:** Conceptualization: M.C., Y.Y., L.L., Y.Z., M.D. and Y.T.; data curation: M.C.; formal analysis: M.C.; methodology: M.C., Y.Y., L.L., Y.Z., M.D. and Y.T.; software: M.C., Y.Y. and L.L.; visualization: M.C. and Y.Y.; writing original draft: M.C. and Y.Y.; writing review and editing: M.C., Y.Y., Y.Z., M.D. and Y.T. All authors have read and agreed to the published version of the manuscript.

**Funding:** This research was funded by the West Light Foundation of the Chinese Academy of Sciences, grant number 2019, National Natural Science Foundation of China, grant numbers 31970223 and 31972858, the Project of the Southeast Asia Biodiversity Research Institute, the Chinese Academy of Sciences, grant number Y4ZK111B01, Transboundary cooperation on biodiversity research and conservation in Gaoligong Mountains, grant number E1ZK251, Yunnan Special Project on Constructing Science and Technology Innovation Center Oriented to South and Southeast Asia, grant number 202303AK140009, the Project of Yunnan Wildlife Conservation, grant number 2023SJ09X-05, the Fund of Key Laboratory for Silviculture and Forest Resources Development of Yunnan Province, Yunnan, Academy of Forestry and Grassland, grant number KFJJ21-05.

**Data Availability Statement:** The original contributions presented in the study are included in the article/supplementary material, further inquiries can be directed to the corresponding author/s.

**Acknowledgments:** The author would like to sincerely thank Jian-Wu Li, Bin Yang, Hong-Bo Ding, Xing-Chi Xie, Qiang Zhang, Quan Yang, Yu-Qiang Chen, Si-Rong Yi, De-Ming He, Guo-Yun Li, Guo-Xing Deng, Dong-Li Quan, and others for their assistance in the collection of *Diplopanax stachyanthus* samples.

**Conflicts of Interest:** The authors declare no conflicts of interest.

## References

1. Rotllan, P.X.; Traveset, A. Declining relict plants: Climate effect or seed dispersal disruption? A landscape-scale approach. *Basic. Appl. Ecol.* **2016**, *17*, 81–91. [\[CrossRef\]](#)
2. Guo, Y.L.; Zhao, Z.F.; Li, X. Moderate warming will expand the suitable habitat of *Ophiocordyceps sinensis* and expand the area of *O. sinensis* with high adenosine content. *Sci. Total Environ.* **2021**, *787*, 147605. [\[CrossRef\]](#)
3. Doxford, S.W.; Freckleton, R.P. Changes in the large-scale distribution of plants: Extinction, colonisation and the effects of climate. *J. Ecol.* **2012**, *100*, 519–529. [\[CrossRef\]](#)
4. Jochum, G.M.; Mudge, K.W.; Thomas, R.B. Elevated temperatures increase leaf senescence and root secondary metabolite concentrations in the understory herb *Panax quinquefolius* (Araliaceae). *Am. J. Bot.* **2007**, *94*, 819–826. [\[CrossRef\]](#) [\[PubMed\]](#)
5. Wei, B.; Wang, R.L.; Hou, K.; Wang, X.Y.; Wu, W. Predicting the current and future cultivation regions of *Carthamus tinctorius* L. using MaxEnt model under climate change in China. *Glob. Ecol. Conserv.* **2018**, *16*, e00477. [\[CrossRef\]](#)
6. Warren, R.; Price, J.; Graham, E.; Forstnerhaeusler, N.; VanDerWal, J. The projected effect on insects, vertebrates, and plants of limiting global warming to 1.5 degrees C rather than 2 degrees C. *Science* **2018**, *360*, 791–795. [\[CrossRef\]](#)
7. Ali, H.; Din, J.U.; Bosso, L.; Hameed, S.; Kabir, M.; Younas, M.; Nawaz, M.A. Expanding or shrinking? Range shifts in wild ungulates under climate change in Pamir-Karakoram mountains, Pakistan. *PLoS ONE* **2021**, *16*, e0260031. [\[CrossRef\]](#) [\[PubMed\]](#)
8. Huang, Z.B.; Xie, L.N.; Wang, H.W.; Zhong, J.B.; Li, Y.C.; Liu, J.L.; Ou, Z.; Liang, X.X.; Li, Y.S.; Huang, H.Y.; et al. Geographic distribution and impacts of climate change on the suitable habitats of Zingiber species in China. *Ind. Crops Prod.* **2019**, *138*, 111429. [\[CrossRef\]](#)
9. Shen, Y.F.; Tu, Z.H.; Zhang, Y.L.; Zhong, W.P.; Xia, H.; Hao, Z.Y.; Zhang, C.G.; Li, H.G. Predicting the impact of climate change on the distribution of two relict Liriodendron species by coupling the MaxEnt model and actual physiological indicators in relation to stress tolerance. *J. Environ. Manag.* **2022**, *322*, 116024. [\[CrossRef\]](#) [\[PubMed\]](#)
10. Zhao, X.M.; Ren, B.P.; Li, D.Y.; Garber, P.A.; Zhu, P.F.; Xiang, Z.F.; Grueter, C.C.; Liu, Z.J.; Li, M. Climate change, grazing, and collecting accelerate habitat contraction in an endangered primate. *Biol. Conserv.* **2019**, *231*, 88–97. [\[CrossRef\]](#)
11. Tiffney, B.H. Perspectives on the origin of the floristic similarity between eastern Asia and eastern North America. *J. Arnold Arbor.* **1985**, *66*, 73–94. [\[CrossRef\]](#)
12. Huang, Y.J.; Jacques, F.M.B.; Su, T.; Ferguson, D.K.; Tang, H.; Chen, W.Y.; Zhou, Z.K. Distribution of Cenozoic plant relicts in China explained by drought in dry season. *Sci. Rep.* **2015**, *5*, 14212. [\[CrossRef\]](#)
13. Qiu, Y.X.; Lu, Q.X.; Zhang, Y.H.; Cao, Y.N. Phylogeography of East Asia's Tertiary relict plants: Current progress and future prospects. *Biodivers. Sci.* **2017**, *25*, 136–146. [\[CrossRef\]](#)
14. Milne, R.; Abbott, R. The origin and evolution of Tertiary relict flora. *Adv. Bot. Res.* **2002**, *38*, 281–314. [\[CrossRef\]](#)
15. Zhekun, Z.; Momohara, A. Fossil history of some endemic seed plants of East Asia and its phytogeographical significance. *Acta Bot. Yunnanica* **2005**, *27*, 449–470.
16. Manchester, S.R.; Chen, Z.D.; Lu, A.M.; Uemura, K. Eastern Asian endemic seed plant genera and their paleogeographic history throughout the Northern Hemisphere. *J. Syst. Evol.* **2009**, *47*, 1–42. [\[CrossRef\]](#)
17. Eyde, R.H. Fossil record and ecology of Nyssa (Cornaceae). *Bot. Rev.* **1997**, *63*, 97–123. [\[CrossRef\]](#)
18. Liu, Y.S.; Basinger, J.F. Fossil Cathaya (Pinaceae) pollen from the Canadian high arctic. *Int. J. Plant Sci.* **2000**, *161*, 829–847. [\[CrossRef\]](#)
19. Heinemann, M. Warm and Sensitive Paleocene-Eocene Climate. Ph.D. Thesis, University of Hamburg, Hamburg, Spain, 2009.
20. Chen, Z.L.; Ding, Z.L. A Review on the Paleocene-Eocene Thermal Maximum. *Quat. Sci.* **2011**, *31*, 937–950. [\[CrossRef\]](#)



21. Jovane, L.G.; Coccioni, R.; Marsili, A.; Acton, G. The late Eocene greenhouse-icehouse transition: Observations from the Massignano global stratotype section and point (GSSP). *Geol. Soc. Am. Spec. Pap.* **2009**, *452*, 149–168.
22. Collinson, M.E.; Hooker, J.J. Paleogene vegetation of Eurasia: Framework for mammalian faunas. *Deinsea* **2003**, *10*, 41–84.
23. Ao, H.; Dupont-Nivet, G.; Rohling, E.J.; Zhang, P.; Ladant, J.B.; Roberts, A.P.; Licht, A.; Liu, Q.S.; Liu, Z.G.; Dekkers, M. Orbital climate variability on the northeastern Tibetan Plateau across the Eocene–Oligocene transition. *Nat. Commun.* **2020**, *11*, 5249. [[CrossRef](#)] [[PubMed](#)]
24. Wang, X.M.; Wang, M.Z.; Zhang, X.Q. Palynology Assemblages and Paleoclimatic Character of the Late Eocene to Early Oligocene in China. *Earth Sci.* **2005**, *30*, 309–316.
25. Chen, C.; Qi, Z.C.; Xu, X.H.; Comes, H.P.; Koch, M.A.; Jin, X.J.; Fu, C.X.; Qiu, Y.X. Understanding the formation of Mediterranean–African–Asian disjunctions: Evidence for Miocene climate-driven vicariance and recent long-distance dispersal in the Tertiary relict *Smilax aspera* (Smilacaceae). *New Phytol.* **2014**, *204*, 243–255. [[CrossRef](#)] [[PubMed](#)]
26. Nie, Z.L.; Sun, H.; Manchester, S.R.; Meng, Y.; Luke, Q.; Wen, J. Evolution of the intercontinental disjunctions in six continents in the *Ampelopsis* clade of the grape family (Vitaceae). *BMC Evol. Biol.* **2012**, *12*, 17. [[CrossRef](#)] [[PubMed](#)]
27. Xie, L.; Wagner, W.L.; Ree, R.H.; Berry, P.E.; Wen, J. Molecular phylogeny, divergence time estimates, and historical biogeography of *Circaea* (Onagraceae) in the Northern Hemisphere. *Mol. Phylogenetics Evol.* **2009**, *53*, 995–1009. [[CrossRef](#)] [[PubMed](#)]
28. Zhang, Q.Y.; Ree, R.H.; Salamin, N.; Xing, Y.W.; Silvestro, D. Fossil-informed models reveal a boreotropical origin and divergent evolutionary trajectories in the walnut family (Juglandaceae). *Syst. Biol.* **2022**, *71*, 242–258. [[CrossRef](#)] [[PubMed](#)]
29. Tiffney, B.H.; Haggard, K.K. Fruits of Mastixioideae (Cornaceae) from the Paleogene of western North America. *Rev. Palaeobot. Palyno* **1996**, *92*, 29–54. [[CrossRef](#)]
30. Eyde, R.H.; Xiang, Q.Y. Fossil Mastixioid (Cornaceae) alive in Eastern Asia. *Am. J. Bot.* **1990**, *77*, 689–692. [[CrossRef](#)]
31. Matthew, K.M. A revision of the genus *Mastixia* (Cornaceae). *Blumea Biodivers. Evol. Biogeogr. Plants* **1976**, *23*, 51–93.
32. He, J.; Zeng, C.J. *Flora of China*; Science Press: Beijing, China, 1978; Volume 54.
33. Sodhi, N.S.; Posa, M.R.C.; Lee, T.M.; Bickford, D.; Koh, L.P.; Brook, B.W. The state and conservation of Southeast Asian biodiversity. *Biodivers. Conserv.* **2010**, *19*, 317–328. [[CrossRef](#)]
34. Stibig, H.J.; Achard, F.; Carboni, S.; Raši, R.; Miettinen, J. Change in tropical forest cover of Southeast Asia from 1990 to 2010. *Biogeosciences* **2014**, *11*, 247–258. [[CrossRef](#)]
35. Deb, J.C.; Phinn, S.; Butt, N.; McAlpine, C.A. Climate change impacts on tropical forests: Identifying risks for tropical Asia. *J. Trop. For. Sci.* **2018**, *30*, 182–194.
36. Estoque, R.C.; Ooba, M.; Avitabile, V.; Hijioka, Y.; DasGupta, R.; Togawa, T.; Murayama, Y.J. The future of Southeast Asia's forests. *Nat. Commun.* **2019**, *10*, 1829. [[CrossRef](#)] [[PubMed](#)]
37. Zhang, X.Y.; Ci, X.Q.; Hu, J.L.; Bai, Y.; Thornhill, A.H.; Conran, J.G.; Li, J. Riparian areas as a conservation priority under climate change. *Sci. Total Environ.* **2023**, *858*, 159879. [[CrossRef](#)]
38. Stockey, R.A.; LePage, B.A.; Pigg, K.B. Permineralized fruits of *Diplopanax* (Cornaceae, Mastixioideae) from the middle Eocene Princeton chert of British Columbia. *Rev. Palaeobot. Palynol.* **1998**, *103*, 223–234. [[CrossRef](#)]
39. Martinetto, E. The first mastixioid fossil from Italy and its palaeobiogeographic implications. *Rev. Palaeobot. Palyno* **2011**, *167*, 222–229. [[CrossRef](#)]
40. Mai, D.H. Entwicklung und klimatische Differenzierung der Laubwaldflora Mitteleuropas im Tertiär. *Flora* **1981**, *171*, 525–582. [[CrossRef](#)]
41. Mai, D.H. On the extinct Mastixiaceae (Cornales) in Europe. *Geophytology* **1993**, *23*, 53–63.
42. Seward, A.C. British Museum (Natural History) The London Clay Flora. *Nature* **1934**, *134*, 6–7. [[CrossRef](#)]
43. Graham, A. *Late Cretaceous and Cenozoic History of North American Vegetation: North of Mexico*; Oxford University Press: Oxford, UK, 1999.
44. Manchester, S.R. Extinct ulmaceous fruits from the Tertiary of Europe and western North America. *Rev. Palaeobot. Palynol.* **1987**, *52*, 119–129. [[CrossRef](#)]
45. Manchester, S.R. Fruits and seeds of the Middle Eocene nut beds flora, Clarno Formation, Oregon. *Paleontographica Am.* **1994**, *58*, 1–205.
46. Brikiatis, L. Late Mesozoic North Atlantic land bridges. *Earth-Sci. Rev.* **2016**, *159*, 47–57. [[CrossRef](#)]
47. Tiffney, B.H.; Manchester, S.R. The use of geological and paleontological evidence in evaluating plant phylogeographic hypotheses in the Northern Hemisphere tertiary. *Int. J. Plant Sci.* **2001**, *162*, S3–S17. [[CrossRef](#)]
48. Czechtz, H.; Skirgiello, A. Dicotyledoneae. *Foss. Flora Turów Near Bogatynia Second. Part Syst. Descr. Plant Remain. No. 4* **1975**, *24*, 25–56.
49. Khan, M.A.; Bera, M.; Spicer, R.A.; Spicer, T.E.V.; Bera, S. First occurrence of mastixioid (Cornaceae) fossil in India and its biogeographic implications. *Rev. Palaeobot. Palyno* **2017**, *247*, 83–96. [[CrossRef](#)]
50. Handel-Mazzetti, H.F.V. Plantae novae Chingianae. *Sinensia* **1933**, *3*, 185–198.
51. Li, Y.L.; Zhu, H.; Yang, J.B. Systematic position of the genus *Mastixia*: Evidence from rbc L gene sequences. *Acta Bot. Yunnanica* **2002**, *24*, 352–358.
52. Zhu, W.H.; Xiang, Q.B. The Origin and Distribution of Genus *Diplopanax* Hand.-Mazz. *J. Nanjing For. Univ.* **2001**, *25*, 35.
53. Averyanov, L.V.; Hiep, N.T. *Diplopanax vietnamensis*, a New Species of Nyssaceae from Vietnam: One More Living Representative of the Tertiary Flora of Eurasia. *Novon* **2002**, *12*, 433–436. [[CrossRef](#)]

54. Ševčík, J.; Kvaček, Z.; Mai, D.H. A new mastixioid florula from tektite-bearing deposits in South Bohemia, Czech Republic (Middle Miocene, Vrábče Member). *Bull. Geosci.* **2007**, *82*, 429–436. [\[CrossRef\]](#)
55. Manchester, S.R.; Collinson, M.E. Mastixioid fruits (Cornales) from the early Eocene London Clay Flora: morphology, anatomy and nomenclatural revision. *Foss. Impr.* **2022**, *78*, 310–328. [\[CrossRef\]](#)
56. Manchester, S.R.; McINTOSH, W.C. Late Eocene silicified fruits and seeds from the John Day Formation near Post, Oregon. *PaleoBios* **2007**, *27*, 7–17.
57. Feng, L.; Xu, Z.Y.; Wang, L. Genetic diversity and demographic analysis of an endangered tree species *Diplopanax stachyanthus* in subtropical China: Implications for conservation and management. *Conserv. Genet.* **2019**, *20*, 315–327. [\[CrossRef\]](#)
58. Khan, M.A.; Spicer, R.A.; Bera, S.; Ghosh, R.; Yang, J.; Spicer, T.E.V.; Guo, S.X.; Su, T.; Jacques, F.M.B.; Grote, P.J. Miocene to Pleistocene floras and climate of the Eastern Himalayan Siwaliks, and new palaeoelevation estimates for the Namling–Oiyug Basin, Tibet. *Glob. Planet. Chang.* **2014**, *113*, 1–10. [\[CrossRef\]](#)
59. IUCN. *Diplopanax stachyanthus*. The IUCN Red List of Threatened Species 1998: E.T32339A9699334. Available online: <https://www.iucnredlist.org/species/32339/9699334> (accessed on 24 March 2024).
60. Fang, X.M.; Yan, M.D.; Zhang, W.L.; Nie, J.S.; Han, W.X.; Wu, F.L.; Song, C.H.; Zhang, T.; Zan, J.B.; Yang, Y.P. Paleogeography control of Indian monsoon intensification and expansion at 41 Ma. *Sci. Bull.* **2021**, *66*, 2320–2328. [\[CrossRef\]](#) [\[PubMed\]](#)
61. Boria, R.A.; Olson, L.E.; Goodman, S.M.; Anderson, R.P. Spatial filtering to reduce sampling bias can improve the performance of ecological niche models. *Ecol. Model.* **2014**, *275*, 73–77. [\[CrossRef\]](#)
62. Hijmans, R.J.; Phillips, S.; Leathwick, J.; Elith, J.; Hijmans, M.R. Package ‘dismo’. *Circles* **2017**, *9*, 1–68.
63. Hijmans, R.J.; Cameron, S.E.; Parra, J.L.; Jones, P.G.; Jarvis, A. Very high resolution interpolated climate surfaces for global land areas. *Int. J. Climatol.* **2005**, *25*, 1965–1978. [\[CrossRef\]](#)
64. Fick, S.E.; Hijmans, R.J. WorldClim 2: New 1-km spatial resolution climate surfaces for global land areas. *Int. J. Climatol.* **2017**, *37*, 4302–4315. [\[CrossRef\]](#)
65. Parding, K.M.; Dobler, A.; McSweeney, C.F.; Landgren, O.A.; Benestad, R.; Erlandsen, H.B.; Mezghani, A.; Gregow, H.; Raty, O.; Viktor, E.; et al. GCMeval-An interactive tool for evaluation and selection of climate model ensembles. *Clim. Serv.* **2020**, *18*, 100167. [\[CrossRef\]](#)
66. Wu, T.W.; Lu, Y.X.; Fang, Y.J.; Xin, X.G.; Li, L.; Li, W.P.; Jie, W.H.; Zhang, J.; Liu, Y.M.; Zhang, L.; et al. The Beijing Climate Center Climate System Model (BCC-CSM): The main progress from CMIP5 to CMIP6. *Geosci. Model. Dev.* **2019**, *12*, 1573–1600. [\[CrossRef\]](#)
67. Chen, G.W.; Ling, J.; Zhang, R.W.; Xiao, Z.N.; Li, C.Y. The MJO From CMIP5 to CMIP6: Perspectives from Tracking MJO Precipitation. *Geophys. Res. Lett.* **2022**, *49*, e2021GL095241. [\[CrossRef\]](#)
68. Lin, L.; Jiang, X.L.; Guo, K.Q.; Byrne, A.; Deng, M. Climate change impacts the distribution of *Quercus* section *Cyclobalanopsis* (Fagaceae), a keystone lineage in East Asian evergreen broadleaved forests. *Plant Divers.* **2023**, *45*, 552–568. [\[CrossRef\]](#) [\[PubMed\]](#)
69. Pearson, R.G.; Raxworthy, C.J.; Nakamura, M.; Peterson, A.T. Predicting species distributions from small numbers of occurrence records: A test case using cryptic geckos in Madagascar. *J. Biogeogr.* **2007**, *34*, 102–117. [\[CrossRef\]](#)
70. Yang, Y.J.W.; Lin, L.; Tan, Y.H.; Deng, M. How Climate Change Impacts the Distribution of *Lithocarpus hancei* (Fagaceae), a Dominant Tree in East Asian Montane Cloud Forests. *Forests* **2023**, *14*, 1049. [\[CrossRef\]](#)
71. Cao, Y.T.; Lu, Z.P.; Gao, X.Y.; Liu, M.L.; Sa, W.; Liang, J.; Wang, L.; Yin, W.; Shang, Q.H.; Li, Z.H. Maximum entropy modeling the distribution area of *Morchella* dill. Ex Pers. species in China under changing climate. *Biology* **2022**, *11*, 1027. [\[CrossRef\]](#)
72. Dormann, C.F.; Elith, J.; Bacher, S.; Buchmann, C.; Carl, G.; Carré, G.; Marquéz, J.R.G.; Gruber, B.; Lafourcade, B.; Leitão, P.J. Collinearity: A review of methods to deal with it and a simulation study evaluating their performance. *Ecography* **2013**, *36*, 27–46. [\[CrossRef\]](#)
73. Naimi, B.; Araújo, M.B. sdm: A reproducible and extensible R platform for species distribution modelling. *Ecography* **2016**, *39*, 368–375. [\[CrossRef\]](#)
74. Allouche, O.; Tsoar, A.; Kadmon, R. Assessing the accuracy of species distribution models: Prevalence, kappa and the true skill statistic (TSS). *J. Appl. Ecol.* **2006**, *43*, 1223–1232. [\[CrossRef\]](#)
75. Wang, Y.S.; Wang, Z.H.; Xing, H.F.; Li, J.W.; Sun, S. Prediction of potential suitable distribution of *Davidia involucreata* Baill in China based on MaxEnt. *Chin. J. Ecol.* **2019**, *38*, 1230–1237. [\[CrossRef\]](#)
76. Yang, J.T.; Jiang, P.; Huang, Y.; Yang, Y.L.; Wang, R.L.; Yang, Y.X. Potential geographic distribution of relict plant *Pteroceltis tatarinowii* in China under climate change scenarios. *PLoS ONE* **2022**, *17*, e0266133. [\[CrossRef\]](#) [\[PubMed\]](#)
77. O'Donnell, J.; Gallagher, R.V.; Wilson, P.D.; Downey, P.O.; Hughes, L.; Leishman, M.R. Invasion hotspots for non-native plants in Australia under current and future climates. *Glob. Chang. Biol.* **2012**, *18*, 617–629. [\[CrossRef\]](#)
78. Zeng, C.Y.; Zhong, Q.J.; Wang, C.Y.; Hu, Y.P.; Wu, M.H.; Meng, W.; Peng, M.C. Ecologically suitable habitats and population characteristics of *Cercidiphyllum japonicum* in China. *Chin. J. Ecol.* **2020**, *39*, 2704–2712. [\[CrossRef\]](#)
79. Liu, Y.; Huang, P.; Lin, F.R.; Yang, W.Y.; Gaisberger, H.; Christopher, K.; Zheng, Y.Q. MaxEnt modelling for predicting the potential distribution of a near threatened rosewood species (*Dalbergia cultrata* Graham ex Benth). *Ecol. Eng.* **2019**, *141*, 105612. [\[CrossRef\]](#)
80. Brown, J.L.; Bennett, J.R.; French, C.M. SDMtoolbox 2.0: The next generation Python-based GIS toolkit for landscape genetic, biogeographic and species distribution model analyses. *PeerJ* **2017**, *5*, e4095. [\[CrossRef\]](#) [\[PubMed\]](#)
81. Guo, Y.K.; Wei, H.Y.; Lu, C.Y.; Gao, B.; Gu, W. Predictions of potential geographical distribution and quality of *Schisandra sphenanthera* under climate change. *PeerJ* **2016**, *4*, e2554. [\[CrossRef\]](#) [\[PubMed\]](#)

82. Callaway, R.M.; Cipollini, D.; Barto, K.; Thelen, G.C.; Hallett, S.G.; Prati, D.; Stinson, K.; Klironomos, J. Novel weapons: Invasive plant suppresses fungal mutualists in America but not in its native Europe. *Ecology* **2008**, *89*, 1043–1055. [\[CrossRef\]](#) [\[PubMed\]](#)
83. Callaway, R.M.; Mahall, B.E.; Wicks, C.; Pankey, J.; Zabinski, C. Soil fungi and the effects of an invasive forb on grasses: Neighbor identity matters. *Ecology* **2003**, *84*, 129–135. [\[CrossRef\]](#)
84. Wang, L.; You, Z.P.; Xu, Y.; Zhang, D.H. Research Status and Endangered Causes of *Diplopanax stachyanthus*. *Bull. Bot. Res.* **2010**, *30*, 344–348.
85. Liu, X.D.; Yin, Z.Y. Sensitivity of East Asian monsoon climate to the uplift of the Tibetan Plateau. *Palaeogeogr. Palaeoclimatol. Palaeoecol.* **2002**, *183*, 223–245. [\[CrossRef\]](#)
86. Zhou, Z.K.; Huang, J.; Ding, W.N. The impact of major geological events on Chinese flora. *Biodivers. Sci.* **2017**, *25*, 123–135. [\[CrossRef\]](#)
87. Yang, Q.; Yuan, M.Q.; Feng, B.X. Study on Community Structure and Resources of Rare Species *Diplopanax stachyanthus* on the Moon Mountain, Rongjiang. *Seed* **2013**, *32*, 55–59. [\[CrossRef\]](#)
88. Zhu, W.H. Systematic Position and Evolution of Genus *Diplopanax stachyanthus* Hand.-Mazz. Doctoral Dissertation, Nanjing Forestry University, Nanjing, China, 1998.
89. Lei, N.F.; Su, Z.X.; Chen, J.S.; Guo, J.H. Germination inhibitors in fruit of rare and endangered *Davidia involucrata*. *Chin. J. Appl. Environ. Biol.* **2003**, *9*, 607–610.
90. Qian, C.M.; Jiang, Z.; Zhou, J.H.; Dai, S.; Su, Y.Y.; Li, S.X. Changes of inhibitory activity during stratification in *Davidia involucrata* seeds. *J. Nanjing For. Univ. Nat. Sci. Ed.* **2016**, *40*, 188–192.
91. Mosbrugger, V.; Utescher, T.; Dilcher, D.L. Cenozoic continental climatic evolution of Central Europe. *Proc. Natl. Acad. Sci. USA* **2005**, *102*, 14964–14969. [\[CrossRef\]](#) [\[PubMed\]](#)
92. Eronen, J.T.; Fortelius, M.; Micheels, A.; Portmann, F.T.; Puolamaki, K.; Janis, C.M. Neogene aridification of the Northern Hemisphere. *Geology* **2012**, *40*, 823–826. [\[CrossRef\]](#)
93. Sunderlin, D.; Loope, G.; Parker, N.E.; Williams, C.J. Paleoclimatic and Paleoecological implications of a Paleocene-Eocene fossil leaf assemblage, Chickaloon formation, Alaska. *Palaios* **2011**, *26*, 335–345. [\[CrossRef\]](#)
94. Taylor, D.W. Paleobiogeographic relationships of angiosperms from the Cretaceous and early Tertiary of the North American area. *Bot. Rev.* **1990**, *56*, 279–417. [\[CrossRef\]](#)
95. Vieira, M.; Poças, E.; Pais, J.; Pereira, D. Pliocene flora from S. Pedro da Torre deposits (Minho, NW Portugal). *Geodiversitas* **2011**, *33*, 71–85. [\[CrossRef\]](#)
96. Zhou, P.; Li, X.Z.; Shi, Z.G.; Sha, Y.Y.; Lei, J.; An, Z.S. Strengthened East Asian Winter Monsoon Regulated by Insolation and Arctic Sea Ice Since the Middle Holocene. *Geophys. Res. Lett.* **2023**, *50*, e2023GL105440. [\[CrossRef\]](#)
97. LePage, B.A.; Yang, H.; Matsumoto, M. The evolution and biogeographic history of *Metasequoia* in the geobiology and ecology of *Metasequoia*. *Geobiol. Ecol. Metasequoia* **2005**, *22*, 3–114. [\[CrossRef\]](#)
98. Lai, W.F.; Shi, C.Y.; Wen, G.W.; Ln, Z.W.; Ye, L.Q.; Huang, Q.L.; Zhang, G.F. Potential impacts of climate change on the distribution of the relict plant *Shaniodendron subaequale*. *Heliyon* **2023**, *9*, e14402. [\[CrossRef\]](#) [\[PubMed\]](#)
99. Tang, C.Q.; Dong, Y.F.; Herrando-Moraira, S.; Matsui, T.; Ohashi, H.; He, L.Y.; Nakao, K.; Tanaka, N.; Tomita, M.; Li, X.S.; et al. Potential effects of climate change on geographic distribution of the Tertiary relict tree species *Davidia involucrata* in China. *Sci. Rep.* **2017**, *7*, 43822. [\[CrossRef\]](#) [\[PubMed\]](#)
100. Wu, J.G.; Lu, J.J. Potential Effects of Climate Change on the Distribution of Dove Trees (*Davidia Involucrata* Baill) in China. *Res. Environ. Sci.* **2009**, *22*, 1371–1381.
101. Wu, X.T.; Wang, M.Q.; Li, X.Y.; Yan, Y.D.; Dai, M.J.; Xie, W.Y.; Zhou, X.F.; Zhang, D.L.; Wen, Y.F. Response of distribution patterns of two closely related species in *Taxus* genus to climate change since last inter-glacial. *Ecol. Evol.* **2022**, *12*, e9302. [\[CrossRef\]](#) [\[PubMed\]](#)
102. Zhang, H.; Zhao, H.X.; Xu, C.G. The potential geographical distribution of *Alsophila spinulosain* under climate change in China. *Chin. J. Ecol.* **2021**, *40*, 968–979. [\[CrossRef\]](#)
103. Zhang, X.Y.; Wei, H.Y.; Zhang, X.H.; Liu, J.; Zhang, Q.Z.; Gu, W. Non-pessimistic predictions of the distributions and suitability of *Metasequoia glyptostroboides* under climate change using a random forest model. *Forests* **2020**, *11*, 62. [\[CrossRef\]](#)
104. Alexander, J.M.; Chalmandrier, L.; Lenoir, J.; Burgess, T.I.; Essl, F.; Haider, S.; Kueffer, C.; McDougall, K.; Milbau, A.; Nuñez, M.A.; et al. Lags in the response of mountain plant communities to climate change. *Glob. Chang. Biol.* **2018**, *24*, 563–579. [\[CrossRef\]](#) [\[PubMed\]](#)
105. Seddon, A.W.R.; Macias, F.M.; Long, P.R.; Benz, D.; Willis, K.J. Sensitivity of global terrestrial ecosystems to climate variability. *Nature* **2016**, *531*, 229–232. [\[CrossRef\]](#) [\[PubMed\]](#)
106. Ernakovich, J.G.; Hopping, K.A.; Berdanier, A.B.; Simpson, R.T.; Kachergis, E.J.; Steltzer, H.; Wallenstein, M.D. Predicted responses of arctic and alpine ecosystems to altered seasonality under climate change. *Glob. Chang. Biol.* **2014**, *20*, 3256–3269. [\[CrossRef\]](#) [\[PubMed\]](#)
107. Rudgers, J.A.; Chung, Y.A.; Maurer, G.E.; Moore, D.I.; Muldavin, E.H.; Litvak, M.E.; Collins, S.L. Climate sensitivity functions and net primary production: A framework for incorporating climate mean and variability. *Ecology* **2018**, *99*, 576–582. [\[CrossRef\]](#) [\[PubMed\]](#)
108. Ge, J.L.; Berg, B.; Xie, Z.Q. Climatic seasonality is linked to the occurrence of the mixed evergreen and deciduous broad—Leaved forests in China. *Ecosphere* **2019**, *10*, e02862. [\[CrossRef\]](#)



109. Song, C.Y.; Liu, H.M.; Gao, J.X. Habitat preference and potential distribution of *Magnolia officinalis* subsp. *officinalis* and *M. o.* subsp. *biloba* in China. *Nat. Conserv. Bulg.* **2019**, *36*, 93–111. [[CrossRef](#)]
110. Guan, X.Y.; Shi, W.; Cao, K.F. Effect of Climate Change in Future on Geographical Distribution of Widespread *Quercus acutissima* and Analysis of Dominant Climatic Factors. *J. Trop. Subtrop. Bot.* **2018**, *26*, 661–668. [[CrossRef](#)]
111. Shi, X.D.; Yin, Q.; Sang, Z.Y.; Zhu, Z.L.; Jia, Z.K.; Ma, L.Y. Prediction of potentially suitable areas for the introduction of *Magnolia wufengensis* under climate change. *Ecol. Indic.* **2021**, *127*, 107762. [[CrossRef](#)]
112. Xu, J.; Deng, M.; Jiang, X.L.; Westwood, M.; Song, Y.G.; Turkington, R. Phylogeography of *Quercus glauca* (Fagaceae), a dominant tree of East Asian subtropical evergreen forests, based on three chloroplast DNA interspace sequences. *Tree Genet. Genomes* **2015**, *11*, 805. [[CrossRef](#)]
113. Song, C.Y.; Liu, H.M. Habitat differentiation and conservation gap of *Magnolia biondii*, *M. denudata*, and *M. sprengeri* in China. *PeerJ* **2019**, *6*, e6126. [[CrossRef](#)]
114. Holbourn, A.E.; Kuhnt, W.; Clemens, S.C.; Kochhann, K.G.D.; Jöhnck, J.; Lübbers, J.; Andersen, N. Late Miocene climate cooling and intensification of southeast Asian winter monsoon. *Nat. Commun.* **2018**, *9*, 1584. [[CrossRef](#)] [[PubMed](#)]
115. Willis, K.J.; Niklas, K.J. The role of Quaternary environmental change in plant macroevolution: The exception or the rule? *Philos. Trans. R. Soc. London B Biol. Sci.* **2004**, *359*, 159–172. [[CrossRef](#)] [[PubMed](#)]
116. Ye, J.W.; Zhang, Y.; Wang, X.J. Phylogeographic history of broad-leaved forest plants in subtropical China. *Acta Ecol. Sin.* **2017**, *37*, 5894–5904. [[CrossRef](#)]
117. Hewitt, G.M. Genetic consequences of climatic oscillations in the Quaternary. *Philos. T R. Soc. B* **2004**, *359*, 183–195. [[CrossRef](#)] [[PubMed](#)]
118. Qian, H.; Ricklefs, R.E. Diversity of temperate plants in east Asia. *Nature* **2001**, *413*, 130. [[CrossRef](#)]
119. Shi, Y. Characteristics of late Quaternary monsoonal glaciation on the Tibetan Plateau and in East Asia. *Quat. Int.* **2002**, *97–98*, 79–91. [[CrossRef](#)]
120. Shi, Y.F.; Ren, B.H.; Wang, J.T.; Edward, D. Quaternary glaciation in China. *Quat. Sci. Rev.* **1986**, *5*, 503–507. [[CrossRef](#)]
121. Tian, Z.; Jiang, D.B. Revisiting last glacial maximum climate over China and East Asian monsoon using PMIP3 simulations. *Palaeogeogr. Palaeoclimatol. Palaeoecol.* **2016**, *453*, 115–126. [[CrossRef](#)]
122. Qian, H.; Ricklefs, R.E. Large-scale processes and the Asian bias in species diversity of temperate plants. *Nature* **2000**, *407*, 180–182. [[CrossRef](#)] [[PubMed](#)]
123. Ricklefs, R.E. A comprehensive framework for global patterns in biodiversity. *Ecol. Lett.* **2004**, *7*, 1–15. [[CrossRef](#)]
124. Tian, Z.P.; Jiang, D.B. Mid-Holocene and last glacial maximum changes in monsoon area and precipitation over China. *Chin. Sci. Bull.* **2015**, *60*, 400–410. [[CrossRef](#)]
125. Zhang, Y.K.; Zhang, S.S. Effects of seed soaking with salicylic acid on seed germination and early seedling growth of *Mastixia euonymoides* under drought stress. *Hunan For. Sci. Technol.* **2022**, *49*, 24–29.
126. Zhang, S.S.; Yuan, C.M.; Chen, J.; Zhang, Y.K. Population Status of Wild *Mastixia euonymoides* as an Extremely Small Population. *For. Inventory Plan.* **2020**, *45*, 82–87.

**Disclaimer/Publisher’s Note:** The statements, opinions and data contained in all publications are solely those of the individual author(s) and contributor(s) and not of MDPI and/or the editor(s). MDPI and/or the editor(s) disclaim responsibility for any injury to people or property resulting from any ideas, methods, instructions or products referred to in the content.